Le Boson H, Séminaire Poincaré XIX (2014) 89 – 107 Séminaire Poincaré

Future Searches on Scalar Boson(s)

Louis FAYARD
LAL - Bât. 200
Université Paris Sud
91898 Orsay cedex, France

Abstract. The discovery of a Brout-Englert-Higgs boson in July 2012 opened the road to new searches in the electroweak symmetry breaking sector, either doing precise measurements of the discovered boson, or looking for additional bosons. This can be done, either at the LHC or at future accelerators that will be described.

1 Introduction

The discovery in July 2012 [1, 2] of a (Brout-Englert-Higgs) BEH boson at the Large Hadron Collider (LHC) [3, 4] ended an era of search of the last piece of the Standard Model, culminating with the Nobel prize given to Englert and Higgs [5, 6] (detailed historical account can be found in [7, 8, 9]). However, even if the Standard Model (SM) agrees with all the experimental data from colliders, it is theoretically unsatisfactory (the hierarchy problem, too many parameters in the Model, ...) and some experimental observations cannot be accomodated (neutrino masses and oscillations, baryon asymmetry in the Universe, dark matter, ...). However no new physics was discovered at the LHC in the run 1 (mainly at a centre of mass energy of 8 TeV). This included Supersymmetry, which is the most popular extension able to accomodate a BEH boson mass close to the one measured [10]. This puts even more pressure to the next runs at the LHC, at a centre of mass energy of 13 or 14 TeV and to the design of the future accelerators. They will be described in the next section and the third section will discuss new physics in the scalar sector, either using the (already discovered) BEH boson as a probe for new physics or trying to find new scalar bosons.

2 Future Facilities

The LHC 'short-term' upgrades will be described first, in subsections 2.1 and 2.2. Then longer term future facilities will be described after. However muon colliders [11], photon colliders [12] and plasma-based particle acceleration [13] will not be described here. General reviews on future facilities can be found elsewhere [14, 15].One can also have a look at the European Strategy [16] and P5 [17] reports or at recent conferences like *Higgs Hunting* [18] or recent ICFA workshops [19].

2.1 Runs 2 and 3 of LHC

The LHC will restart in the middle of 2015 at a centre of mass energy of 13 TeV (and maybe later 14 TeV) and will work during run 2 and run 3 (up to about 2022) at a luminosity close to $\sim 2\ 10^{34}\text{cm}^{-2}s^{-1}$. The run 2 will last about 3 years with $\sim 50\ \text{fb}^{-1}$ each year and will be followed after a long shutdown (LS2) of $\sim$ one year by the run 3 with $\sim 60\ \text{fb}^{-1}$ each year [20].

2.2 High-Luminosity LHC (HL-LHC)

After 10 years of operation, the performance of the LHC in terms of integrated luminosity will saturate. This is the main motivation to propose a High-Luminosity LHC (HL-LHC) [21, 22, 23], starting around 2025 and aiming at accumulate every year of HL-LHC the same total luminosity that could be obtained in the previous decade, i.e 300 fb^{-1}. The guidelines are to have an accelerator able to reach $2\ 10^{35}\text{cm}^{-2}s^{-1}$, but to run in the initial part of the fill by luminosity levelling in the initial part of the fill at $5\ 10^{34}\text{cm}^{-2}s^{-1}$(see Figure 1). This allows one to reach the integrated luminosity without having too large pile-up in the experiments at the beginning of the run. The main modifications, in addition to the new injector LINAC4 that should be connected in 2019 are:

- Crab cavities to take advantage of the small β^*;
- cryo-collimators and high field (Nb_3Sn) 11 T dipoles in dispersion suppressors (at least close to ALICE);
- new high field (Nb_3Sn)/larger aperture interaction region magnets (in ATLAS and CMS. The current triplet assembly (mainly the orbit corrector magnets) will reach the end of their lifetime due to radiation damage at an integrated luminosity of ca. 300 fb^{-1}.

One should note that some 11 T (Nb_3Sn) dipoles have already been tested at Fermilab. Additional information about HL-LHC can be found in the recent ECFA workshop [24].

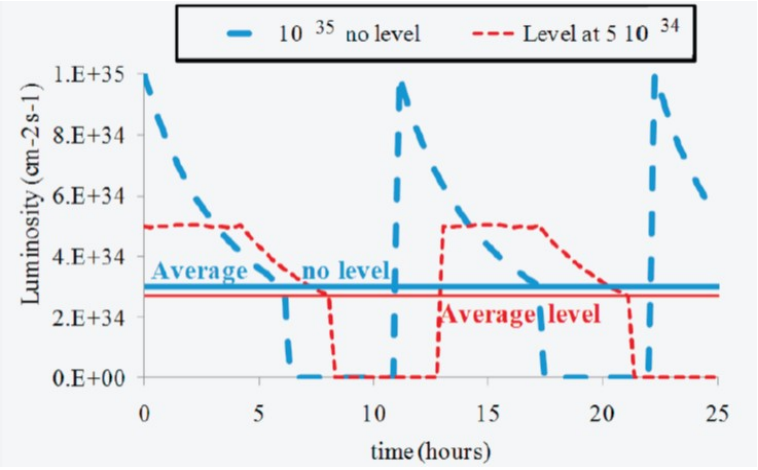

Figure 1: Luminosity levelling principle [11].

2.3 Linear Colliders

The Linear Collider Collaboration [25] is an organisation that brings the two most likely candidates, the Compact Linear Collider Study (CLIC) and the International Linear Collider (ILC), together under one roof.

2.3.1 The International Linear Collider (ILC)

The International Linear Collider (ILC) is a high-luminosity linear electron-positron collider based on 1.3 GHz superconducting radio-frequency (SCRF) accelerating technology. Its centre-of-mass-energy range is 200 $\sim$ 500 GeV (extendable to 1TeV). A schematic view of the accelerator complex, indicating the location of the major sub-systems [26, 27, 28, 29, 30] is shown on Figure 2. and a more detailed layout on Figure 3.

One sees on the schematic layout:

- A polarised electron source based on a photocathode DC gun;
- a polarised positron source in which positrons are obtained from electron-positron pairs by converting high-energy photons produced by passing the high-energy main electron beam through an undulator;
- 5 GeV electron and positron damping rings (DR) with a circumference of 3.2 km, housed in a common tunnel;
- beam transport from the damping rings to the main linacs, followed by a two-stage bunchcompressor system prior to injection into the main linac.
- two 11 km main linacs, utilising 1.3 GHz SCRF cavities operating at an average gradient of 31.5 MV/m, with a pulse length of 1.6 ms;
- two beam-delivery systems, each 2.2 km long, which bring the beams into collision with a 14 mrad crossing angle, at a single interaction point which can be occupied by two detectors in a so-called push-pull configuration.

A summary table of the parameters can be found on Figure 4. One should emphasize the synergy between the ILC and the European X-ray Free Electron Laser (XFEL)[31] which is currently under construction at DESY and will begin operation soon.

2.3.2 The Compact Linear Collider (CLIC)

An overview of the CLIC layout can be found on Figure 5. CLIC [33, 34, 32, 35] is based on high gradient normal-conducting accelerating structures where the RF power for the acceleration of the colliding beams is extracted from a high-current Drive Beam that runs parallel with the main linac. The focus of CLIC Research and Development over the last years has been on addressing a set of key feasibility issues that are essential for proving the fundamental validity of the CLIC concept. Several larger system tests have been performed to validate the two-beam scheme, and of particular importance are the results from the CLIC test facility at CERN

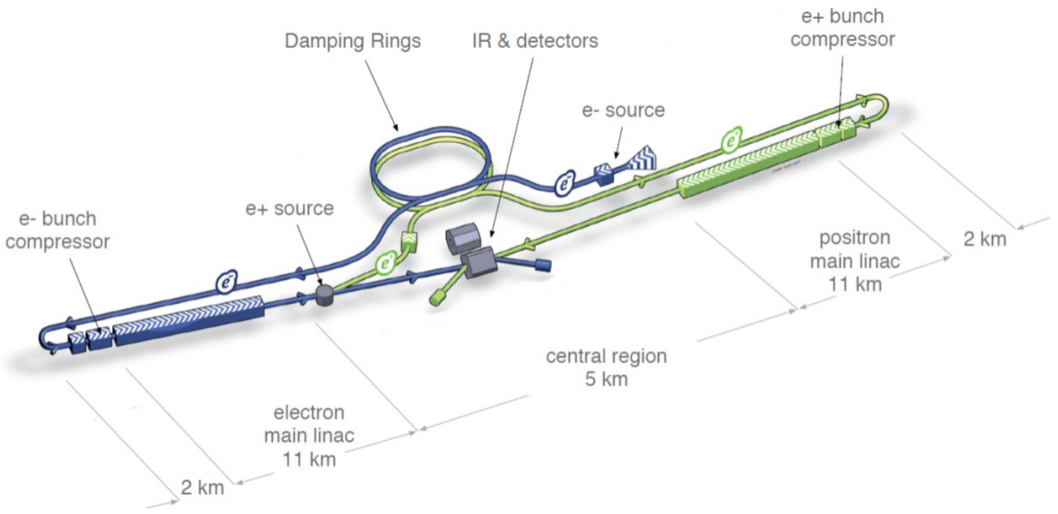

Figure 2: Schematic layout of the ILC, indicating all the major subsystems (not to scale) [26].

(CTF3) which have demonstrated the two-beam acceleration at gradients exceeding 100 MV/m.The CLIC accelerator can be built in energy stages, as shown in Figure 6, re-using the existing equipment for each new stage. At each energy stage the centre of mass energy can be tuned to lower values within a range of approximately a factor three with limited loss in luminosity performance. The ultimate choice of the CLIC energy stages will be driven by the physics aims, where further input from LHC data, in particular 14 TeV data, is expected. The recent LHC Higgs discovery makes an initial energy stage around 350 GeV to 375 GeV very attractive, but final choices will depend on further LHC findings. CLIC main parameters can be found in Figure 7. The yearly energy and power consumption is shown in Figure 8.

2.4 Future Circular Colliders

CERN is undertaking an integral design study for post-LHC particle accelerator options in a global context. The Future Circular Collider (FCC) [36] puts an emphasis on proton-proton and electron-positron (lepton) high-energy frontier machines.
This study is exploring the potential of hadron and lepton circular colliders, performing an in-depth analysis of infrastructure and operation concepts and considering the technology research and development programs that would be required to build a future circular collider. A conceptual design report will be delivered before the end of 2018 in time for the next update of the European Strategy for Particle Physics. Here we will not discuss FCC-he, High-Energy LHC (HL-LHC) [21] or LHeC [37, 38].

2.4.1 FCC-hh

Circular proton-proton colliders are the main, and possibly only, tool available for exploring particle physics in the energy range of tens of TeV.

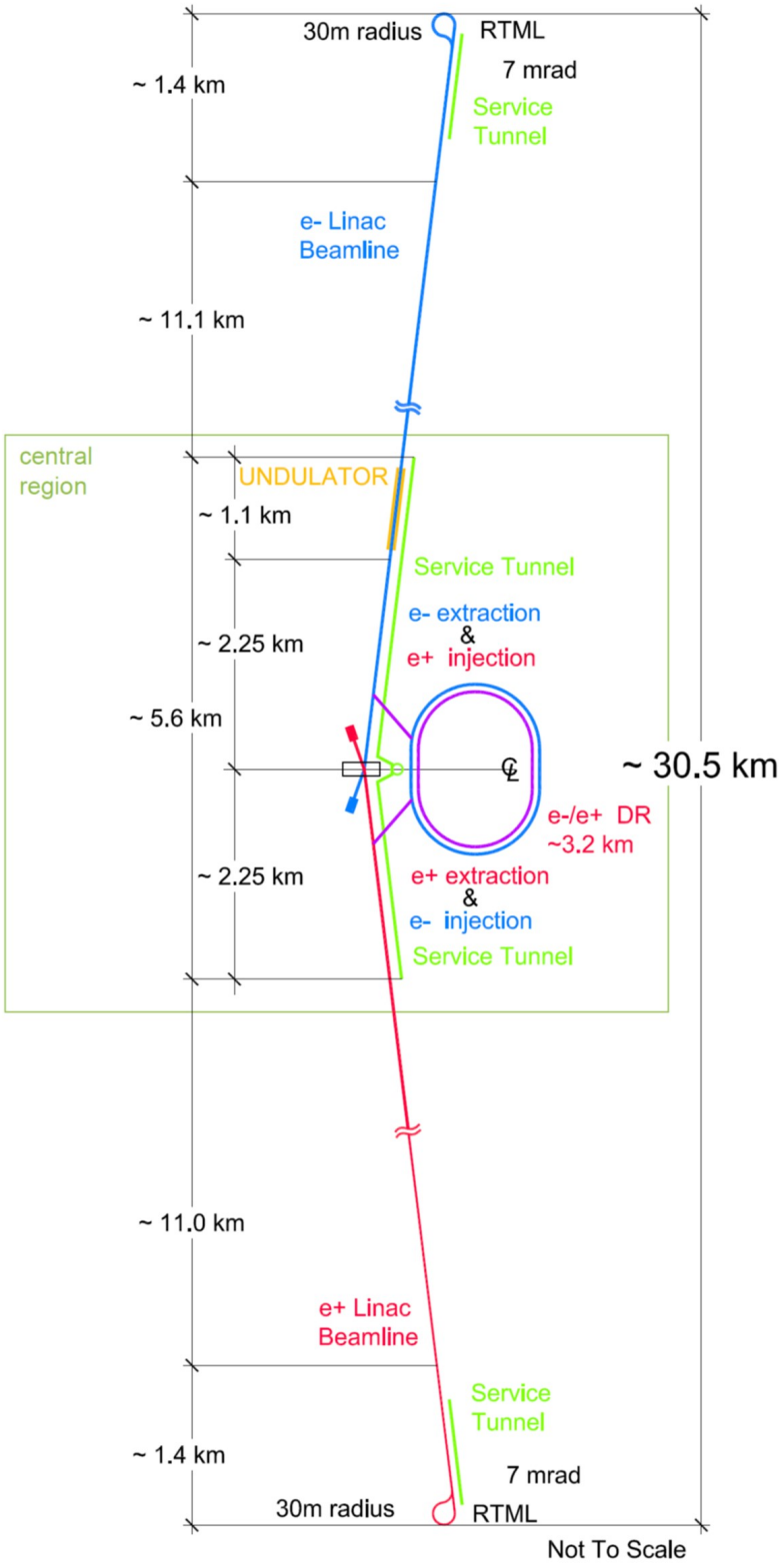

Figure 3: Layout of the ILC complex at $\sqrt{s} = 0.5$ TeV [29].

			Baseline 500 GeV Machine			1st Stage	L Upgrade	E_{CM} Upgrade	
Centre-of-mass energy	E_{CM}	GeV	250	350	500	250	500	A 1000	B 1000
Collision rate	f_{rep}	Hz	5	5	5	5	5	4	4
Electron linac rate	f_{linac}	Hz	10	5	5	10	5	4	4
Number of bunches	n_b		1312	1312	1312	1312	2625	2450	2450
Bunch population	N	$\times 10^{10}$	2.0	2.0	2.0	2.0	2.0	1.74	1.74
Bunch separation	Δt_b	ns	554	554	554	554	366	366	366
Pulse current	I_{beam}	mA	5.8	5.8	5.8	5.8	8.8	7.6	7.6
Main linac average gradient	G_a	MV m^{-1}	14.7	21.4	31.5	31.5	31.5	38.2	39.2
Average total beam power	P_{beam}	MW	5.9	7.3	10.5	5.9	21.0	27.2	27.2
Estimated AC power	P_{AC}	MW	122	121	163	129	204	300	300
RMS bunch length	σ_z	mm	0.3	0.3	0.3	0.3	0.3	0.250	0.225
Electron RMS energy spread	$\Delta p/p$	%	0.190	0.158	0.124	0.190	0.124	0.083	0.085
Positron RMS energy spread	$\Delta p/p$	%	0.152	0.100	0.070	0.152	0.070	0.043	0.047
Electron polarisation	P_-	%	80	80	80	80	80	80	80
Positron polarisation	P_+	%	30	30	30	30	30	20	20
Horizontal emittance	$\gamma\epsilon_x$	µm	10	10	10	10	10	10	10
Vertical emittance	$\gamma\epsilon_y$	nm	35	35	35	35	35	30	30
IP horizontal beta function	β_x^*	mm	13.0	16.0	11.0	13.0	11.0	22.6	11.0
IP vertical beta function	β_y^*	mm	0.41	0.34	0.48	0.41	0.48	0.25	0.23
IP RMS horizontal beam size	σ_x^*	nm	729.0	683.5	474	729	474	481	335
IP RMS veritcal beam size	σ_y^*	nm	7.7	5.9	5.9	7.7	5.9	2.8	2.7
Luminosity	L	$\times 10^{34}$ cm^{-2}s^{-1}	0.75	1.0	1.8	0.75	3.6	3.6	4.9
Fraction of luminosity in top 1%	$L_{0.01}/L$		87.1%	77.4%	58.3%	87.1%	58.3%	59.2%	44.5%
Average energy loss	δ_{BS}		0.97%	1.9%	4.5%	0.97%	4.5%	5.6%	10.5%
Number of pairs per bunch crossing	N_{pairs}	$\times 10^3$	62.4	93.6	139.0	62.4	139.0	200.5	382.6
Total pair energy per bunch crossing	E_{pairs}	TeV	46.5	115.0	344.1	46.5	344.1	1338.0	3441.0

Figure 4: Summary table of the 250 $\sim$ 500 GeV baseline and luminosity and energy upgrade parameters. Also included is a possible 1st stage 250 GeV parameter set (half the original main linac length) [26].

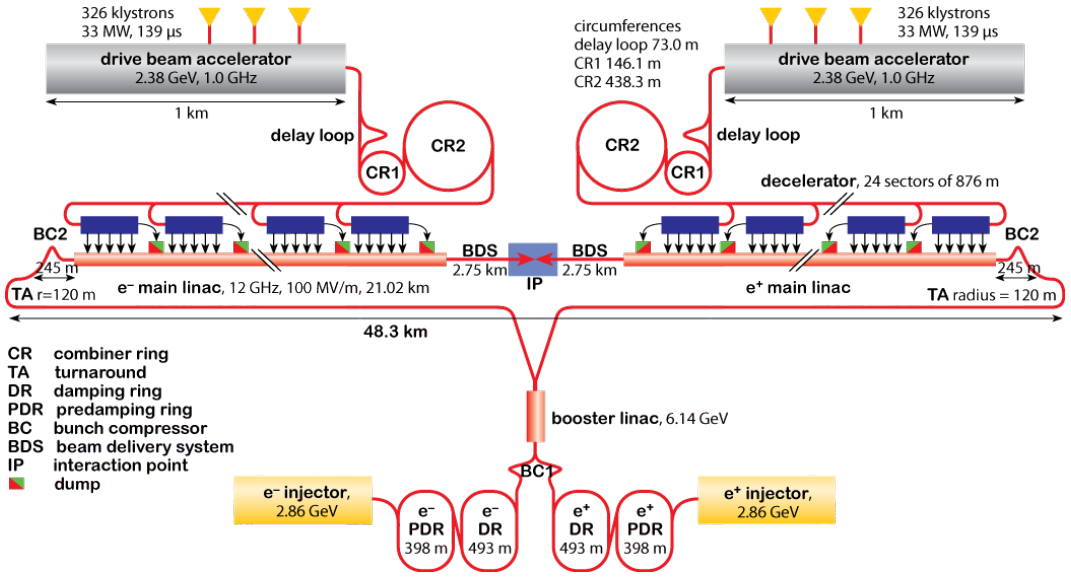

Figure 5: Overview of the CLIC layout at $\sqrt{s} = 3$ TeV [32].

Parameter	Symbol	Unit	Stage 1	Stage 2	Stage 3
Center-of-mass energy	$\sqrt{s}$	GeV	350	1400	3000
Integrated luminosity	$\mathscr{L}_{\text{int}}$	ab^{-1}	0.5	1.5	2.0

Figure 6: Center of mass energy and assumed integrated luminosity for the different CLIC machine stages [35]. The integrated luminosities correspond each to four or five years of operation of a fully commissioned machine running 200 days per year with an effective up-time of 50%.

Description [units]	**500 GeV**	**3 TeV**
Total (peak 1%) luminosity	$2.3\ (1.4)\times10^{34}$	$5.9\ (2.0)\times10^{34}$
Total site length [km]	13.0	48.4
Loaded accel. gradient [MV/m]	80	100
Main Linac RF frequency [GHz]	12	
Beam power/beam [MW]	4.9	14
Bunch charge [10^9 e^+/e^-]	6.8	3.72
Bunch separation [ns]	0.5	
Bunch length [μm]	72	44
Beam pulse duration [ns]	177	156
Repetition rate [Hz]	50	
Hor./vert. norm. emitt. [$10^{-6}/10^{-9}$m]	2.4/25	0.66/20
Hor./vert. IP beam size [nm]	202/2.3	40/1
Beamstrahlung photons/electron	1.3	2.2
Hadronic events/crossing at IP	0.3	3.2
Coherent pairs at IP	200	6.8×10^8

Figure 7: CLIC main parameters for centre of mass energies of 500 GeV and 3 TeV [33].

	Power [MW]	**Days**	**Energy** [TWh]
Nominal operation mode	582	177	2.47
Fault-induced downtime	60	44	0.06
Programmed stops	60	144	0.21
Energy consumption per year			2.74

Figure 8: Yearly energy and power consumption for the nominal 3 TeV CLIC [33].

The bending radius ρ of a relativistic particle of charge e and momentum p is related to the magnetic field of strength B by $p = eB\rho$. Therefore the energy of pp collisions can be raised by increasing the strength of the dipole magnets, or the bending radius ρ, and, thereby, the ring circumference. The proton-proton FCC collider (FCC-hh) design combines both approaches. Specifically, the FCC ring circumference of about 100 km would enable pp collisions of 50 TeV in the centre of mass with the present 8.3 T LHC magnets (made with NbTi superconductor), of 100 TeV with 16 T magnets and of 125 GeV with 20 T magnets. The main technological challenge is therefore magnets: one should replace the magnets. Nb_3Sn superconductor can reach a proactical magnetic field up to 15 T and, as discussed above, few Nb_3Sn magnets are planned for HL-LHC, which will represent an important milestone towards the FCC. High Temperature Superconductor (HTS) materials, like yttrium copper oxyde YBCO could be used in an hybrid coil design in order to get up to 20 T. A sketch of such a magnet is shown on Figure 9. One should note that there are very important

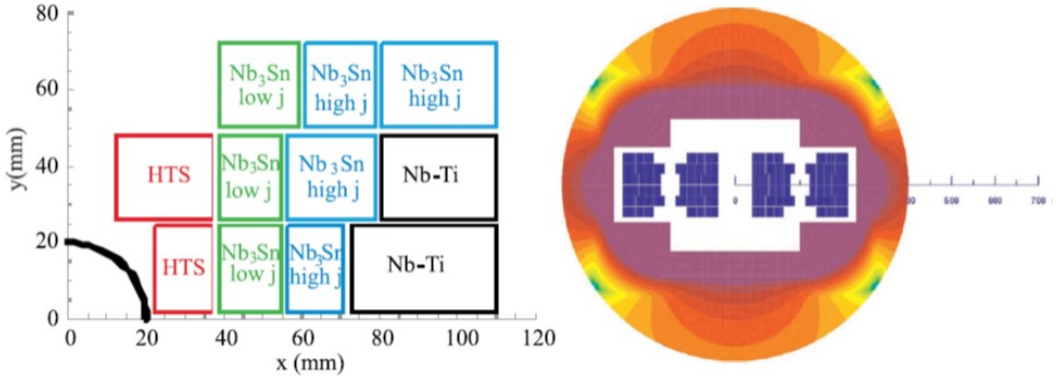

Figure 9: Sketch of cross section of a 20 T magnet with hybrid coil [21]

technological challenges here, as shown on Figure 10 where the progress of accelerator magnets for hadron colliders is shown.

2.4.2 FCC-ee

The discovery of a BEH boson at an energy reachable by a collider slightly more energetic than LEP2, together with the excellent performance of the two B factories PEP-II and KEKB, have led to new proposals [39, 40, 41] for a next generation e^+e^- collider. In order to serve as a BEH factory such a collider needs to be able to operate at at least a centre of mass energy of 240 GeV (for efficient $e^+e^- \to ZH$ production), i.e 15% above the LEP2 peak energy. Reaching even higher energies,e.g up to 350 GeV centre of mass, for $t\bar{t}$ production, or even maybe 500 GeV for Zhh and $t\bar{t}h$ studies, might be possible for a new ring of larger circumference. The preliminary power consumption is estmated to be about 300 MW at 350 GeV centre of mass [40, 15].

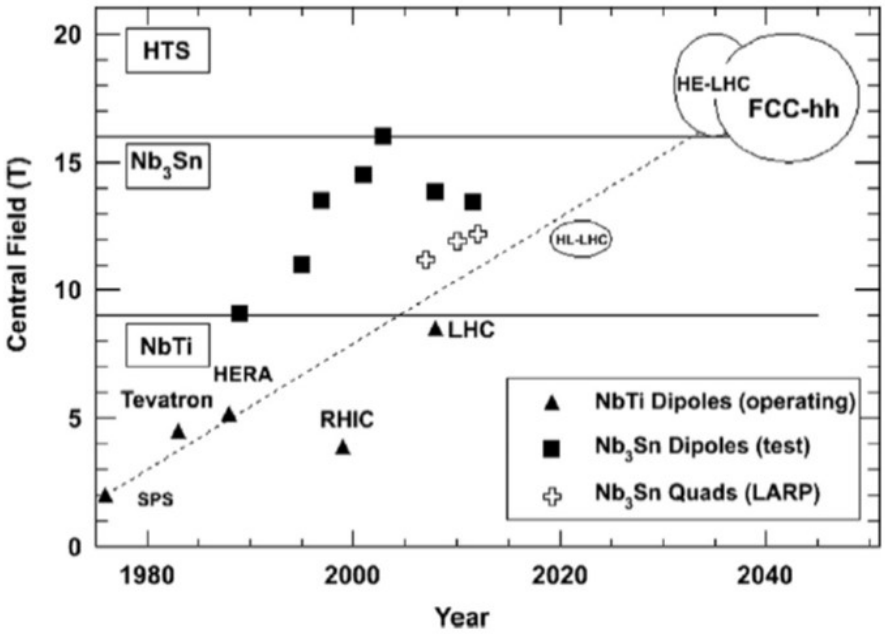

Figure 10: Progress of accelerator magnets for hadron colliders [23].

2.4.3 CepC

China is currently thinking to an e^+e^- collider, where the current design, CepC [42, 43], is a single ring collider two times larger than LEP. It can be associated with a 30-50 TeV proton collider, called SppC.

2.4.4 Comparison of various proposals

One can find in Figure 11 the comparison of various parameters. Projected e^+e^- luminosities can be found in Figure 12.

3 New physics in the scalar sector

Only new physics in the scalar sector will be described rapidly here. Discussions of new physics outside the scalar sector can be found in reports of each future facilities or elsewhere (for HL-LHC see [44, 45]). One can look at reviews of the BEH boson inside [46] and outside [47, 48, 49] the Standard Model. It is outside the scope of this article to give details. I just remind that the most economical low-energy supersymmetric extension of the SM is the Minimal Supersymmetric Standard Model (MSSM) which is itself one of the 2HDM, 2 (BE)Higgs Doublet Models. Five physical bosons are left in the spectrum, one charged pair $H^{\pm}$, one CP-odd scalar, A, and two CP-even states, H and h. There are two free parameters at the tree level, which can be taken as M_A and $\tan\beta$. Deviations from the SM are often parametrized as scale factors (κ) of BEH couplings relative to their SM values [50].

parameter	LHC (pp) design	FCC-hh	LEP2 achieved	FCC-ee (TLEP) Z	Z (cr. w.)	W	H	$t\bar{t}$	CepC
species	pp	pp	e^+e^-	e^+e^-	e^+e^-	e^+e^-	e^+e^-	e^+e^-	e^+e^-
$E_{\rm beam}$ [GeV]	7,000	50,000	104	45.5	45	80	120	175	120
circumf. [km]	26.7	100	26.7	100	100	100	100	100	54
current [mA]	584	500	3.0	1450	1431	152	30	6.6	16.6
no. of bunches, n_b	2808	10600	4	16700	29791	4490	1360	98	50
N_b [10^{11}]	1.15	1.0	4.2	1.8	1.0	0.7	0.46	1.4	3.7
ϵ_x [nm]	0.5	0.04	22	29	0.14	3.3	0.94	2	6.8
ϵ_y [pm]	500	41	250	60	1	7	2	2	20
β_x^* [m]	0.55	1.1	1.2	0.5	0.5	0.5	0.5	1.0	0.8
β_y^* [mm]	550	1100	50	1	1	1	1	1	1.2
σ_x^* [μm]	16.7	6.8	162	121	8	26	22	45	74
σ_y^* [μm]	16.7	6.8	3.5	0.25	0.032	0.13	0.044	0.045	0.16
θ_c [mrad]	0.285	0.074	0	0	30	0	0	0	0
$f_{\rm rf}$ [MHz]	400	400	352	800	300	800	800	800	700
$V_{\rm rf}$ [GV]	0.016	>0.020	3.5	2.5	0.54	4	5.5	11	6.87
α_c [10^{-5}]	32	11	14	18	2	2	0.5	0.5	4.15
$\delta_{\rm rms}^{\rm SR}$ [%]	—	—	0.16	0.04	0.04	0.07	0.10	0.14	0.13
$\sigma_{z,\rm rms}^{\rm SR}$ [mm]	—	—	11.5	1.64	1.9	1.01	0.81	1.16	2.3
$\delta_{\rm rms}^{\rm tot}$ [%]	0.003	0.004	0.16	0.06	0.12	0.09	0.14	0.19	0.16
$\sigma_{z,\rm rms}^{\rm tot}$ [mm]	75.5	80	11.5	2.56	6.4	1.49	1.17	1.49	2.7
F_{hg}	1.0	1.0	0.99	0.64	0.94	0.79	0.80	0.73	0.61
$\tau_{\|\|}$ [turns]	10^9	10^7	31	1320	1338	243	72	23	40
ξ_x/IP	0.0033	0.005	0.04	0.031	0.032	0.060	0.093	0.092	0.103
ξ_y/IP	0.0033	0.005	0.06	0.030	0.175	0.059	0.093	0.092	0.074
no. of IPs, n_{IP}	3 (4)	2 (4)	4	4	4	4	4	4	2
L/IP [10^{34}/cm^2/s]	1	5	0.01	28	219	12	6	1.7	1.8
$\tau_{\rm beam}$ [min]	2760	1146	300	287	38	72	30	23	57
$P_{\rm SR}$/beam [MW]	0.0036	2.4	11	50	50	50	50	50	50
energy / beam [MJ]	392	8400	0.03	22	22	4	1	0.4	0.3

Figure 11: Parameters of the Proposed FCC-hh, FCC-ee/TLEP and CepC, Compared with LEP2 and the LHC Design [15].

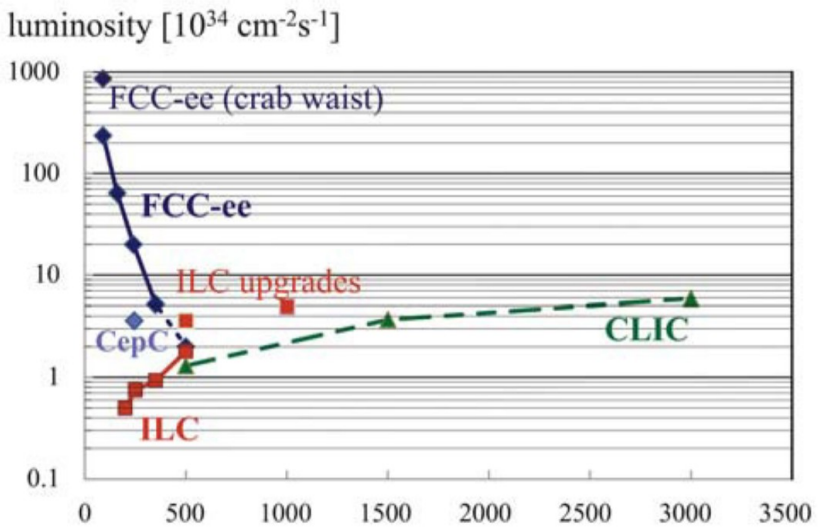

Figure 12: Projected total electron-positron luminosities vs. c.m. energy for various proposed colliders [15]. The luminosities of FCC-ee and CepC are summed respectively over 4 or 2 IPs.

In general the size of couplings modifications from the SM values is of the order of few % when new physics is at a scale of 1 TeV [51]. and decreases when the new physics scale increases. This set the scale for the uncertainties that one aims.
Tests of new physics in the BEH sector can be done, either by studying the decays of the already discovered boson, or looking at new bosons.
Detectors will not be described here, but information can be found in the reports associated to the facilities.

3.1 Next runs of the LHC

One can find more information in recent workshops [24] or reviews [52, 53]. One sees in Figure 13 and 14 the expected precisions from CMS [45] on the measurements of the signal strengths (ratio of the cross section divided by the SM predicted cross section) and on the coupling scale factors κ. Extrapolations are presented under two uncertainty scenarios. In Scenario 1, all systematic uncertainties are left unchanged. In Scenario 2, the theoretical uncertainties are scaled by a factor of 1/2, while other systematic uncertainties are scaled by the square root of the integrated luminosity. The comparison of the two uncertainty scenarios indicates a range of possible future measurements.

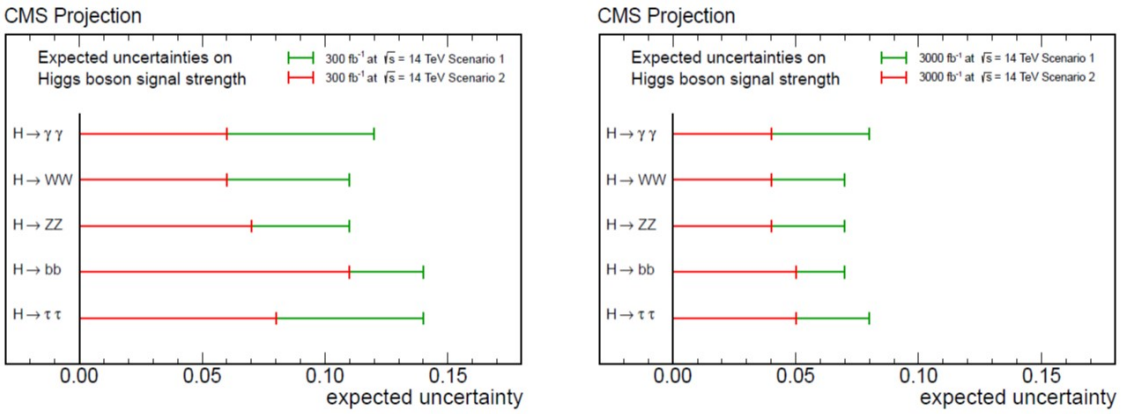

Figure 13: Estimated precision on the measurements of the signal strength for a SM-like BEH boson. The projections assume $\sqrt{s} = 14$ TeV and an integrated dataset of 300 fb^{-1} (left) and 3000 fb^{-1} (right). The projections are obtained with the two uncertainty scenarios described in the text [45].

Figure 15, from ATLAS [54], shows the relative uncertainty on the signal strenth μ defined as the ratio of the measured cross section by the SM cross section for various BEH decay final states. The uncertainties are quite good.
Some tests on additional bosons of the BEH sector can also be done, looking at $A/H \to \tau\tau$, $A/H \to t\bar{t}$ $A \to Zh$, $H \to hh$, $H \to ZZ$.

Studies are presented on the prospects for the observation of Higgs pair production in the channel $H \to \gamma\gamma$ $H \to b\bar{b}$ using an upgraded ATLAS detector, assuming a dataset comprising 3000 fb^{-1} of 14 TeV proton-proton collisions at the High-Luminosity LHC (HL-LHC). Generator-level Monte Carlo events are used to

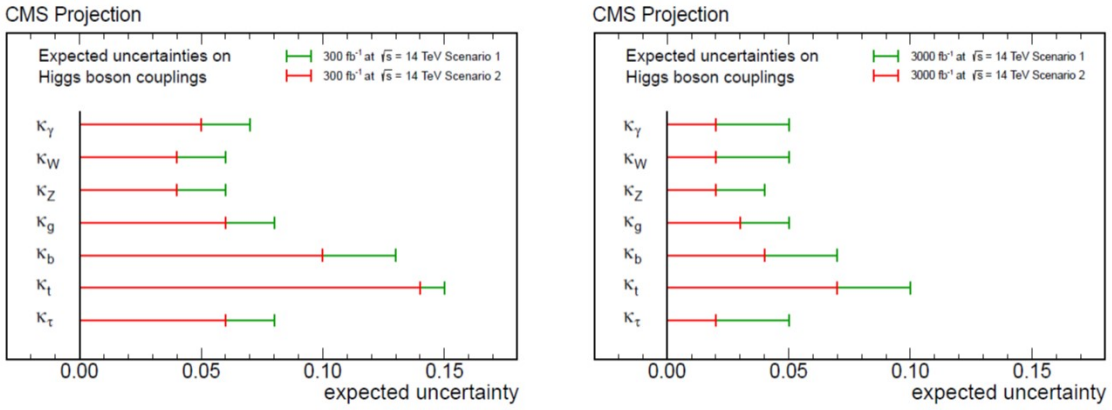

Figure 14: Estimated precision on the measurements of the couplings for a SM-like BEH boson. The projections assume $\sqrt{s} = 14$ TeV and an integrated dataset of 300 fb^{-1} (left) and 3000 fb^{-1} (right). The projections are obtained with the two uncertainty scenarios described in the text [45].

perform this study, with parameterised efficiencies and resolution applied to approximate the expected performance of the upgraded ATLAS detector under HL-LHC conditions. After event selection, a signal yield of around 8 events is obtained for the Standard Model scenario, corresponding to a signal significance of 1.3 standard deviation [55].

3.2 FCC-hh

Figure 16 summarises the increase in rate for several BEH production channels in pp collisions,as a function of the centre of mass energy, covering various ranges of possibilities that are curently discussed. Final states with the largest invariant mass (like tth and hh) benefit the most from the energy increase.

3.3 e^+e^- colliders

The cross sections as a function of the centre of mass energy are shown in Figure 17. A key production mode is $e^+e^- \to Zh$ where events can be detected inclusively, completely independent of the BEH decay mode by tagging the Z via $Z \to e^+e^-$ or $\mu^+\mu^-$ and requiring that the recoil mass is consistent with the BEH mass. The normalisation of this rate allows a precise measurement of the coupling of the Z to the BEH boson. One can then obtain *absolute* measurements of *all* possible branching ratios and the BEH total width.

The various couplings of the BEH boson to different particles can be obtained in e^+e^- colliders with very good precisions. For instance Figure 18 shows the results of a *full* ILC program. Expected accuracies are also shown in Figure 19 and are very good.

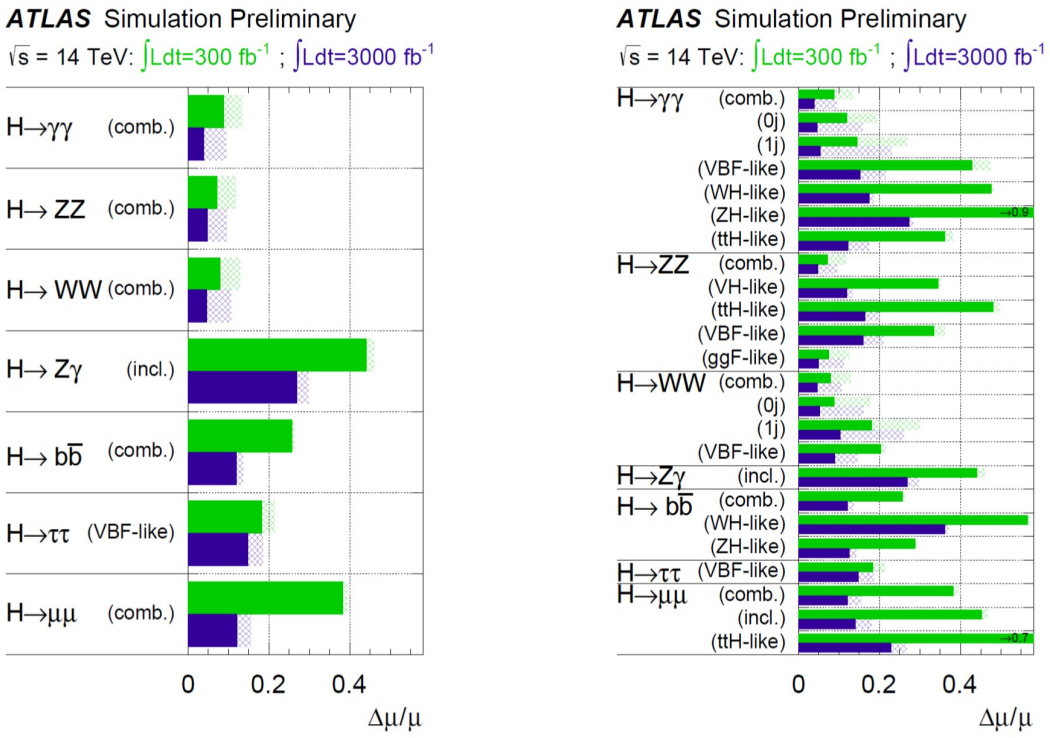

Figure 15: Relative uncertainty on the signal strength μ for all Higgs final states considered in this note in the different experimental categories used in the combination, assuming a SM BEH boson with a mass of 125 GeV expected with 300 fb^{-1} and 3000 fb^{-1} 14 TeV LHC data. The uncertainty pertains to the number of events passing the experimental selection, not to the particular BEH boson process targeted. The hashed areas indicate the increase of the estimated error due to current theory systematic uncertainties. The abbreviation (comb.) indicates that the precision on μ is obtained from the combination of the measurements from the different experimental sub-categories for the same final state, while (incl.) indicates that the measurement from the inclusive analysis was used. The left side shows only the combined signal strength in the considered final states, while the right side also shows the signal strength in the main experimental sub-categories within each final state [54].

Process	σ (14 TeV)	R (33)	R (40)	R (60)	R (80)	R (100)
gg→H	50.4 pb	3.5	4.6	7.8	11	15
qq→qqH	4.40 pb	3.8	5.2	9.3	14	19
q$\bar{q}$→WH	1.63 pb	2.9	3.6	5.7	7.7	10
q$\bar{q}$→ZH	0.90 pb	3.3	4.2	6.8	10	13
pp→HH	33.8 fb	6.1	8.8	18	29	42
pp→ttH	0.62 pb	7.3	11	24	41	61

Figure 16: Evolution of the cross-sections for different BEH production processes in pp collisions with centre of mass energy. The cross-sections at a centre of mass energy of 14 TeV is shown in the second column,and the ratios between the cross sections at the considered centre of mass energy and 14 TeV are shown in the following columns. All rates assume a BEH mass of 125GeV and SM couplings [23].

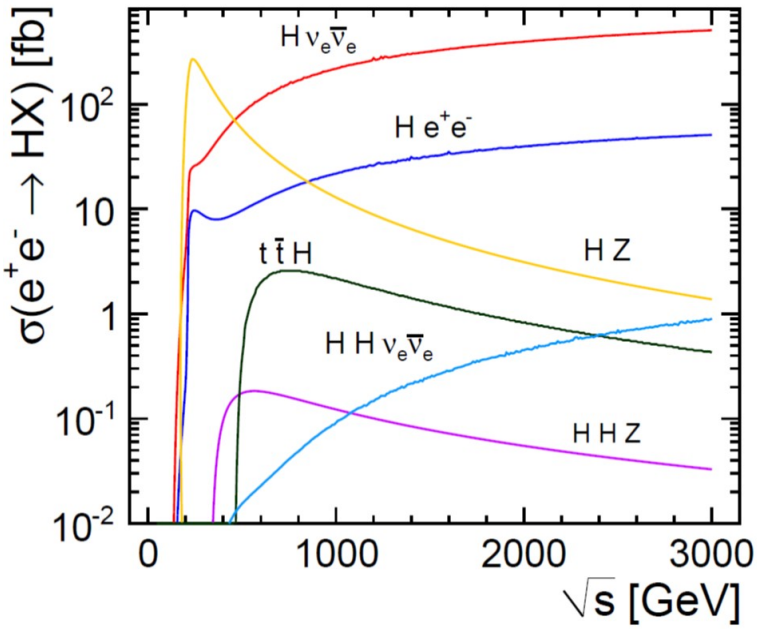

Figure 17: The center-of-mass dependencies of the cross sections for the main Higgs production processes at an e^+e^- collider. The values shown correspond to unpolarized beams and do not include the effects of initial-stare radiation (ISR) or beamstrahlung [35].

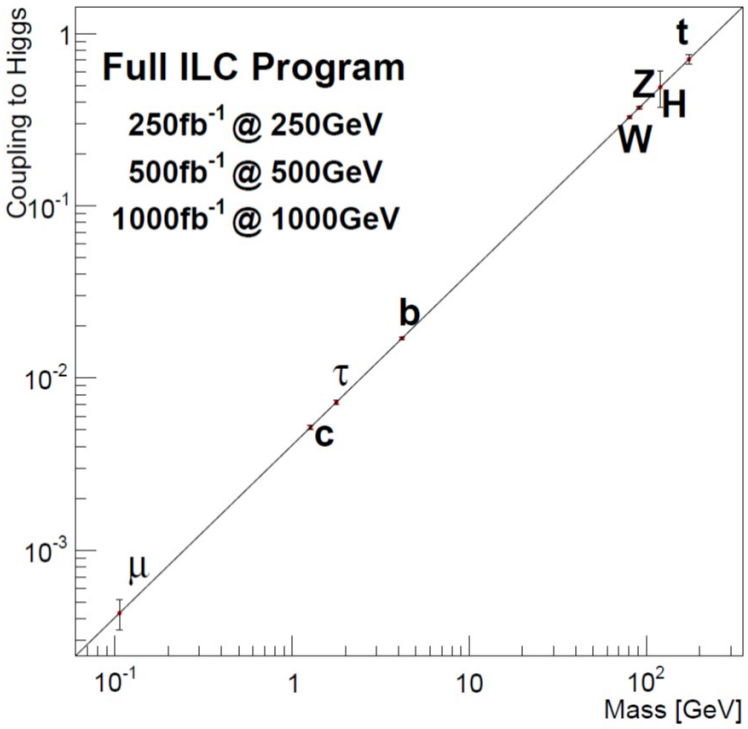

Figure 18: Expected precision from the full ILC program of tests of the Standard Model prediction that the BEH coupling to each particle is proportional to its mass [27].

Mode	LHC	ILC(250)	ILC500	ILC(1000)
WW	4.1 %	1.9 %	0.24 %	0.17 %
ZZ	4.5 %	0.44 %	0.30 %	0.27 %
$b\bar{b}$	13.6 %	2.7 %	0.94 %	0.69 %
gg	8.9 %	4.0 %	2.0 %	1.4 %
$\gamma\gamma$	7.8 %	4.9 %	4.3 %	3.3 %
$\tau^+\tau^-$	11.4 %	3.3 %	1.9 %	1.4 %
$c\bar{c}$	–	4.7 %	2.5 %	2.1 %
$t\bar{t}$	15.6 %	14.2 %	9.3 %	3.7 %
$\mu^+\mu^-$	–	–	–	16 %
self	–	–	104%	26 %
BR(invis.)	$< 9\%$	< 0.44 %	< 0.30 %	< 0.26 %
$\Gamma_T(h)$	20.3%	4.8 %	1.6 %	1.2 %

Figure 19: Expected accuracies for Higgs boson couplings. For the invisible branching ratio, the numbers quoted are 95% confidence upper limits. The four columns refer to: LHC, 300 fb^{-1}, 1 detector; ILC at 250 GeV, with 250 fb^{-1}; ILC at 500 GeV, with 500 fb^{-1}; ILC at 1000 GeV, with 1000 fb^{-1}. Each column includes the stated data set and all previous ones [27].

3.4 Comparisons

Expected predictions on the BEH couplings are shown in Figure 20 and match the required uncertainties.

Facility	LHC	HL-LHC	ILC500	ILC500-up	ILC1000	ILC1000-up	CLIC	TLEP (4 IPs)
$\sqrt{s}$ (GeV)	14,000	14,000	250/500	250/500	250/500/1000	250/500/1000	350/1400/3000	240/350
$\int \mathcal{L}dt$ (fb^{-1})	300/expt	3000/expt	250+500	1150+1600	250+500+1000	1150+1600+2500	500+1500+2000	10,000+2600
κ_γ	5 – 7%	2 – 5%	8.3%	4.4%	3.8%	2.3%	–/5.5/<5.5%	1.45%
κ_g	6 – 8%	3 – 5%	2.0%	1.1%	1.1%	0.67%	3.6/0.79/0.56%	0.79%
κ_W	4 – 6%	2 – 5%	0.39%	0.21%	0.21%	0.2%	1.5/0.15/0.11%	0.10%
κ_Z	4 – 6%	2 – 4%	0.49%	0.24%	0.50%	0.3%	0.49/0.33/0.24%	0.05%
κ_ℓ	6 – 8%	2 – 5%	1.9%	0.98%	1.3%	0.72%	3.5/1.4/<1.3%	0.51%
$\kappa_d = \kappa_b$	10 – 13%	4 – 7%	0.93%	0.60%	0.51%	0.4%	1.7/0.32/0.19%	0.39%
$\kappa_u = \kappa_t$	14 – 15%	7 – 10%	2.5%	1.3%	1.3%	0.9%	3.1/1.0/0.7%	0.69%

Figure 20: Expected precisions on the Higgs couplings and total width from a constrained 7-parameter fit assuming no non-SM production or decay modes.The fit assumes generation universality (the couplings for u, c, t (d, s, b and e, μ, τ) are identical). The ranges shown for LHC and HL-LHC represent the conservative and optimistic scenarios for systematic and theory uncertainties. ILC numbers assume $(e^-; e^+)$ polarizations of (-0.8; -0.3) at 250 and 500 GeV and (-0.8; 0.2) at 1000 GeV, plus a 0.5% theory uncertainty. CLIC numbers assume polarizations of (-0.8; 0) for energies above 1 TeV. TLEP numbers assume unpolarized beams [51].

4 Conclusions

One hopes to have interesting results in the next runs of the LHC (runs 2 and 3, and, after 2025, HL-LHC). The longer term future should also provide major tests of physics outside the Standard Model in the scalar sector, with e^+e^- (circular or linear) colliders or pp colliders.

Acknowledgements

I thank D. Delgove for his help. I thank also G. Arduini, P. Bambade, A. Blondel, O. Bruning, J.-B. De Vivie, A. Djouadi, A. Falkowski, C. Grojean, I. Laktineh, L. Linssen, L. Mapelli, L. Nisati, D. Schulte, J. Wenninger and F. Zimmermann for discussions.

References

[1] G. Aad *et al.* [ATLAS Collaboration], "Observation of a new particle in the search for the Standard Model Higgs boson with the ATLAS detector at the LHC," Phys. Lett. B **716**, 1 (2012) [arXiv:1207.7214 [hep-ex]].

[2] S. Chatrchyan *et al.* [CMS Collaboration], "Observation of a new boson at a mass of 125 GeV with the CMS experiment at the LHC," Phys. Lett. B **716**, 30 (2012) [arXiv:1207.7235 [hep-ex]].

[3] O. Bruning, H. Burkhardt and S. Myers, "The large hadron collider," Prog. Part. Nucl. Phys. **67**, 705 (2012).

[4] L. Evans and P. Bryant, "LHC Machine," JINST **3**, S08001 (2008).

[5] F. Englert, "The BEH mechanism and its scalar boson," Annalen Phys. **526**, 201 (2014).

[6] P. W. Higgs, "Evading the Goldstone theorem," Annalen Phys. **526**, 211 (2014).

[7] [Royal Swedish Academy of Sciences Collaboration], "The BEH-mechanism, interactions with short range forces and scalar particles," AAPPS Bulletin **23**, 6, 3 (2013).

[8] S. Weinberg, "The Making of the standard model," Eur. Phys. J. C **34**, 5 (2004), [hep-ph/0401010].

[9] N. Andari, "Observation of a BEH-like boson decaying into two photons with the ATLAS detector at the LHC," CERN-THESIS-2012-144, LAL12-300.

[10] N. Craig, "The State of Supersymmetry after Run I of the LHC," arXiv:1309.0528 [hep-ph].

[11] Y. Alexahin, C. M. Ankenbrandt, D. B. Cline, A. Conway, M. A. Cummings, V. Di Benedetto, E. Eichten and C. Gatto *et al.*, "Muon Collider Higgs Factory for Snowmass 2013," arXiv:1308.2143 [hep-ph].

[12] V. I. Telnov, "Comments on photon colliders for Snowmass 2013," arXiv:1308.4868 [physics.acc-ph].

[13] S. M. Hooker, "Developments in laser-driven plasma accelerators," Nature Photon. **7**, 775 (2013), [arXiv:1406.5118 [physics.plasm-ph]].

[14] A. Blondel, A. Chao, W. Chou, J. Gao, D. Schulte and K. Yokoya, "Report of the ICFA Beam Dynamics Workshop 'Accelerators for a Higgs Factory: Linear vs. Circular' (HF2012)," arXiv:1302.3318 [physics.acc-ph].

[15] F. Zimmermann, M. Benedikt, D. Schulte and J. Wenninger, "Challenges for Highest Energy Circular Colliders," IPAC-2014-MOXAA01.

[16] http://council.web.cern.ch/council/en/EuropeanStrategy/ESParticlePhysics.html.

[17] http://www.usparticlephysics.org/p5/.

[18] http://higgshunting.fr.

[19] 11th ICFA Seminar in Beijing (october 2014), http://indico.ihep.ac.cn/conferenceOtherViews.py?view=standard\&confId=3867.

[20] S. Myers, "Summary of the RLIUP Workshop, Archamps 29th - 31st October 2013", https://indico.cern.ch/event/281478/overview.

[21] E. Todesco, M. Lamont and L. Rossi, "High luminosity LHC and high energy LHC," Proceedings, CMS Workshop: Perspectives on Physics and on CMS at Very High Luminosity, HL-LHC: Alushta, Crimea, Ukraine, May 2831, 2012.

[22] G. Arduini, "LHC Machine Upgrade," IFD2014, INFN Workshop on Future Detectors for HL-LHC, Trento, http://events.unitn.it/en/ifd2014.

[23] W. Barletta, M. Battaglia, M. Klute, M. Mangano, S. Prestemon, L. Rossi and P. Skands, "Future hadron colliders: From physics perspectives to technology Research and Development," Nucl. Instrum. Meth. A **764**, 352 (2014).

[24] ECFA High Luminosity LHC Experiments Workshop - 2014 (october 2014), https://indico.cern.ch/event/315626/other-view?view=standard.

[25] https://www.linearcollider.org.

[26] T. Behnke, J. E. Brau, B. Foster, J. Fuster, M. Harrison, J. M. Paterson, M. Peskin and M. Stanitzki *et al.*, "The International Linear Collider Technical Design Report - Volume 1: Executive Summary," arXiv:1306.6327 [physics.acc-ph].

[27] H. Baer, T. Barklow, K. Fujii, Y. Gao, A. Hoang, S. Kanemura, J. List and H. E. Logan *et al.*, "The International Linear Collider Technical Design Report - Volume 2: Physics," arXiv:1306.6352 [hep-ph].

[28] C. Adolphsen, M. Barone, B. Barish, K. Buesser, P. Burrows, J. Carwardine, J. Clark and H. M. Durand *et al.*, "The International Linear Collider Technical Design Report - Volume 3.I: Accelerator & in the Technical Design Phase," arXiv:1306.6353 [physics.acc-ph].

[29] C. Adolphsen, M. Barone, B. Barish, K. Buesser, P. Burrows, J. Carwardine, J. Clark and H. M. Durand *et al.*, "The International Linear Collider Technical Design Report - Volume 3.II: Accelerator Baseline Design," arXiv:1306.6328 [physics.acc-ph].

[30] T. Behnke, J. E. Brau, P. N. Burrows, J. Fuster, M. Peskin, M. Stanitzki, Y. Sugimoto and S. Yamada *et al.*, "The International Linear Collider Technical Design Report - Volume 4: Detectors," arXiv:1306.6329 [physics.ins-det]. INSPIRE as of 02 Nov 2014.

[31] M. Altarelli, R. Brinkmann, M. Chergui, W. Decking, B. Dobson, S. Dusterer, G. Grubel and W. Graeff *et al.*, "XFEL: The European X-Ray Free-Electron Laser. Technical design report," DESY-06-097.

[32] P. Lebrun, L. Linssen, A. Lucaci-Timoce, D. Schulte, F. Simon, S. Stapnes, N. Toge and H. Weerts *et al.*, "The CLIC Programme: Towards a Staged e+e- Linear Collider Exploring the Terascale: CLIC Conceptual Design Report," arXiv:1209.2543 [physics.ins-det].

[33] M. Aicheler, M. Aicheler, P. Burrows, M. Draper, T. Garvey, P. Lebrun, K. Peach and N. Phinney *et al.*, "A Multi-TeV Linear Collider Based on CLIC Technology: CLIC Conceptual Design Report," CERN-2012-007, SLAC-R-985, KEK-Report-2012-1, PSI-12-01, JAI-2012-001.

[34] L. Linssen, A. Miyamoto, M. Stanitzki and H. Weerts, "Physics and Detectors at CLIC: CLIC Conceptual Design Report," arXiv:1202.5940 [physics.ins-det], Nov 2014.

[35] H. Abramowicz *et al.* [CLIC Detector and Physics Study Collaboration], "Physics at the CLIC e+e- Linear Collider – Input to the Snowmass process 2013," arXiv:1307.5288 [hep-ex].

[36] http://cern.ch/fcc.

[37] J. L. Abelleira Fernandez, C. Adolphsen, P. Adzic, A. N. Akay, H. Aksakal, J. L. Albacete, B. Allanach and S. Alekhin *et al.*, "A Large Hadron Electron Collider at CERN," arXiv:1211.4831 [hep-ex].

[38] J. L. Abelleira Fernandez *et al.* [LHeC Study Group Collaboration], "A Large Hadron Electron Collider at CERN: Report on the Physics and Design Concepts for Machine and Detector," J. Phys. G **39**, 075001 (2012), [arXiv:1206.2913 [physics.acc-ph]].

[39] A. Blondel and F. Zimmermann, "A High Luminosity e^+e^- Collider in the LHC tunnel to study the Higgs Boson," arXiv:1112.2518.

[40] M. Koratzinos, A. P. Blondel, R. Aleksan, O. Brunner, A. Butterworth, P. Janot, E. Jensen and J. Osborne *et al.*, "TLEP: A High-Performance Circular e^+e^- Collider to Study the Higgs Boson," arXiv:1305.6498 [physics.acc-ph].

[41] M. Bicer *et al.* [TLEP Design Study Working Group Collaboration], "First Look at the Physics Case of TLEP," JHEP **1401**, 164 (2014), [arXiv:1308.6176 [hep-ex]].

[42] http://cepc.ihep.ac.cn.

[43] X. C. Lou, " The CEPC-SppC Study Group in China, CFHEP Kick-off Meeting, Beijing", http://beijingcenterfuturecollider.wikispaces.com/events.

[44] [ATLAS Collaboration], "Search for Supersymmetry at the high luminosity LHC with the ATLAS experiment ATL-PHYS-PUB-2014-010".

[45] [CMS Collaboration], "Projected Performance of an Upgraded CMS Detector at the LHC and HL-LHC: Contribution to the Snowmass Process," arXiv:1307.7135.

[46] A. Djouadi, "The Anatomy of electro-weak symmetry breaking. I: The Higgs boson in the standard model," Phys. Rep. **457**, 1 (2008), [hep-ph/0503172].

[47] A. Djouadi, "The Anatomy of electro-weak symmetry breaking. II. The Higgs bosons in the minimal supersymmetric model," Phys. Rept. **459**, 1 (2008), [hep-ph/0503173].

[48] D. Rainwater, "Searching for the Higgs boson," hep-ph/0702124.

[49] G. C. Branco, P. M. Ferreira, L. Lavoura, M. N. Rebelo, M. Sher and J. P. Silva, "Theory and phenomenology of two-Higgs-doublet models," Phys. Rep. **516**, 1 (2012), [arXiv:1106.0034 [hep-ph]].

[50] A. David *et al.* [LHC Higgs Cross Section Working Group Collaboration], "LHC HXSWG interim recommendations to explore the coupling structure of a Higgs-like particle," arXiv:1209.0040 [hep-ph].

[51] S. Dawson, A. Gritsan, H. Logan, J. Qian, C. Tully, R. Van Kooten, A. Ajaib and A. Anastassov *et al.*, "Working Group Report: Higgs Boson," arXiv:1310.8361 [hep-ex].

[52] A. G. Holzner [for the ATLAS and CMS Collaborations], "Beyond standard model Higgs physics: prospects for the High Luminosity LHC," arXiv:1411.0322 [hep-ex].

[53] M. Vidal [CMS Collaboration], "Future prospects of Higgs Physics at CMS," arXiv:1409.1711 [hep-ex].

[54] [ATLAS Collaboration], "Projections for measurements of Higgs boson signal strengths and coupling parameters with the ATLAS detector at a HL-LHC, ATL-PHYS-PUB-2014-016 ".

[55] [ATLAS Collaboration], "Prospects for measuring Higgs pair production in the channel $H \to \gamma\gamma$ $H \to b\bar{b}$ using the ATLAS detector at the HL-LHC, ATL-PHYS-PUB-2014-019 ".